



# Characterisation of ZnS nanocrystals prepared by wet chemical method

W Shambhunath Singh<sup>a\*</sup>, N Shanta Singh<sup>a</sup>, Ajay Soni<sup>c</sup>, S Dorendrajit Singh<sup>b</sup>  
L Robindro Singh<sup>b</sup> and Gunadhor S Okram<sup>c</sup>

<sup>a</sup>Department of Physics, Manipur College, Imphal-795 008, Manipur, India

<sup>b</sup>Department of Physics, Manipur University, Canchipur, Imphal-795 003, Manipur, India

<sup>c</sup>UGC-DAE Consortium for Scientific Research, Indore-452 017, Madhya Pradesh, India

E-mail : snath1@sancharnet.in

Received 1 March 2007, accepted 7 September 2007

**Abstract** : ZnS nanocrystals of different sizes have been prepared by wet chemical method. X-Ray diffraction (XRD) pattern of ZnS powder shows the zinc blende structure of the crystals with a size variation from 2.9 to 1.6 nm with the addition of capping agent  $C_2H_5OSH$ . The optical absorption of ZnS deposited on quartz shows the blue shift with the increase in the bandgap from 3.6 to 4.0 eV. The observed low thermal activation energy of 0.4 eV determined from resistivity data on the pellets of capped ZnS suggests the formation of charge carrier traps in the presence of capping agent. Thermoluminescence (TL) glow curves of the nanostructured ZnS crystals could not be observed.

**Keywords** : Nanostructures, semiconductors, chemical synthesis, optical properties

**PACS Nos.** : 81.07.Bc, 78.67.Bf

## 1. Introduction

Group II-VI semiconductors occupy a prominent place in the semiconductor physics and optoelectronic devices as they show a high efficiency of radiative recombination, high absorption co-efficient and direct band gaps corresponding to a wide spectrum of wavelengths from ultraviolet to infra-red regions. Since the theoretical explanation of the quantum confinement effect of zero dimensional nanomaterials or quantum dots by Efros and Efros [1] and their novel properties and potential applications [2] these materials have drawn the interests of many researchers in recent years. Special attention is paid to

nanocrystalline semiconductors for their remarkable properties such as nanoelectronics, quantum electronics, sensor technology, non-linear optics and solar technology, different from their conventional counterparts [3].

Among II-VI semiconductors CdS and ZnS are widely used as window layers of solar cells. They exhibit strong size-dependent optical properties. Increase in the band gap and hence the blue shift in the optical absorbance with decrease in the particle size is observed. This effect occurs when the size of the nanocrystals is smaller than the corresponding bulk Bohr exciton radius, a consequence of localisation of charge carriers and hence quantum confinement [4]. Extensive investigations [5–17] have been carried out on II-VI semiconductor nanomaterials as they are relatively easy to synthesise and can generally be prepared as nanoparticles, or in thin film forms. Among a number of methods for the preparation of ZnS wet chemical synthesis process offers an inexpensive and simple means to synthesise such particles with good control of size and size distribution by optimising various parameters and can be deposited over a large area. Many workers [18–21] reported the use of using  $\text{NH}_4\text{OH}$  as complexing agent of Zn to form  $[\text{Zn}(\text{NH}_3)_4]^{2+}$ , which ensures the slow release of  $\text{Zn}^{2+}$  ions from the complex during the reaction. It also can vary the pH of the reaction bath.

In this paper we present the preparation of nanostructured ZnS crystals using wet chemical method using inorganic precursors  $\text{ZnCl}_2$  and  $\text{Na}_2\text{S}$  as the sources of Zn and S respectively. Mercaptoethanol ( $\text{C}_2\text{H}_5\text{OSH}$ ) and liquor ammonia in form of  $\text{NH}_4\text{OH}$  have been used as capping agent and complexing agent respectively. XRD pattern of the prepared ZnS powder shows that with the addition of  $\text{C}_2\text{H}_5\text{OSH}$  the size of ZnS decreases from 2.9 nm to 1.6 nm. The size of the particles has also been calculated using effective mass approximation (EMA). The blue shift has been observed in the absorbance spectra of ZnS thin films deposited on quartz by normal dip coating with the addition of  $\text{C}_2\text{H}_5\text{OSH}$ . This is due to the quantum confinement effect. The band gap calculated using the absorbance spectra increases from 3.6 to 4.0 eV. Chen *et al* [12, 13] reported thermoluminescence (TL) glow curve of ZnS nanocrystals and studied the surface states of the nanoparticles. They have pointed out that electron or hole traps are produced in the band gaps of the nanocrystals even without irradiation since in such particles, ions at the surface increase rapidly when the size becomes smaller. Carriers (electrons or holes) trapped in such surface states or defect states may be released by thermal stimulation and recombine at recombination centers to give out TL. Further, the observed TL of nanocrystalline ZnS samples has been attributed to the long wavelength peak in the absorbance spectrum and hence to the presence of surface states. However, Kumbhojkar *et al* [9] could not observe any red shifted peak in the absorption spectra of ZnS. Indeed, for deeper understanding on ZnS nanocrystals, their electrical properties in the low temperature are also desirable. So far, this has been mostly reported for high temperatures [22,23]. In this paper low temperature resistivity of ZnS prepared with and without capping agent over a range of temperature 150 to 300 K has been measured. ZnS prepared without capping agent remains as an insulator over this range of temperature whereas ZnS prepared with  $\text{C}_2\text{H}_5\text{OSH}$  shows a transition at around 250 K giving a thermal activation energy of 0.4 eV

which is an indication of charge carrier traps. The thermoluminescence (TL) readout of ZnS nanocrystals before and after irradiation by  $\gamma$ -rays has been recorded. However no TL of ZnS nanocrystal could be observed.

## 2. Experimental details

The preparation method reported by Qu *et al* [17] has been modified with the addition of  $\text{NH}_4\text{OH}$ . The ZnS samples are prepared using  $\text{ZnCl}_2$  (GR, Merck) and  $\text{Na}_2\text{S}$  (GR, Merck) as sources of Zn and S respectively. Liquor ammonia (30% GR, Merck) is added to 100 ml of freshly prepared  $\text{ZnCl}_2$  (0.1 M) solution. The solution becomes turbid initially but on adding excess ammonia the solution becomes clear as before indicating the formation of the complex  $[\text{Zn}(\text{NH}_3)_4]^{2+}$ .  $\text{NH}_4\text{Cl}$  is used as buffer solution. Following the standard method [18], the chemically and ultrasonically cleaned quartz and glass substrates are mounted in the reaction bath before the addition of  $\text{Na}_2\text{S}$ . The mixture is then heated upto  $70^\circ\text{C}$  and 0.1 M  $\text{Na}_2\text{S}$  is added at the rate of 1 ml per minute under nitrogen atmosphere with constant stirring. The reaction is carried out using different molarities of the capping agent  $\text{C}_2\text{H}_5\text{OSH}$ . Thin films of ZnS are thus deposited on quartz and glass substrates by dip coating method. Further, the reaction is continued to obtain the precipitate of ZnS. The precipitate is centrifuged, washed with distilled water several times to extract any excess  $\text{Na}_2\text{S}$ , and finally extracted with methanol. The precipitates of ZnS are air-dried at  $40^\circ\text{C}$ . ZnS nanocrystals thus prepared without capping agent is labeled as Z1, with  $\text{C}_2\text{H}_5\text{OSH}$  (0.001 M) as Z2 and  $\text{C}_2\text{H}_5\text{OSH}$  (0.05 M) as Z3.

The particle size and crystal structure of the samples are determined from XRD data obtained using Rigaku 18 kW Rotating X-ray generator equipped with Rigaku D-Max-300,  $\theta - 2\theta$  Goniometer with  $\text{CuK}_\alpha$  X-radiation. The ionic composition is determined using energy dispersive X-rays (EDX) data. The micrographs are recorded using a Digital Instruments Nanoscope AFM (E Version-245). The optical absorbance of ZnS deposited on quartz is recorded using UV-Visible Spectrophotometer (Systronics-2202). The TL readout data of ZnS nanocrystals before and after  $\gamma$ -rays irradiation has been recorded using a TL recorder (RCA931A). The resistivity data are collected on the pellets of 8 mm diameter of dried ZnS with the help of a Keithley 6517A electrometer and a 240 Lakeshore temperature controller in the temperature range 150 K to 300 K.

## 3. Results and discussion

The XRD patterns of nanostructured ZnS powders Z1, Z2 and Z3 indicate that the crystallites exist in the zinc blende structure (Figure 1) with prominent peaks at the  $2\theta$  values of  $28.75^\circ$ ,  $48.05^\circ$  and  $57.17^\circ$  corresponding to (111), (220) and (311) planes respectively [JCPDS Card No. 80-0020]. Close observation of the patterns shows gradual broadening of the peaks, say (111) peak. These peaks have been utilised to estimate the size of the crystallites using Scherrer formula [24],  $D = K\lambda/(\beta \cos \theta)$ , where  $D$  is the average grain size,  $K$  is a constant ( $\sim 1$ ),  $\beta$  is the full width at half maximum and  $\theta$  is the Bragg's angle. The crystallite sizes thus estimated for the Z1, Z2 and Z3 samples are in decreasing

order (Table 1) Figure 2 shows a representative 2-dimensional AFM picture of the pellet of Z2. The nanostructured particles are seen to be agglomerated to form a grain having a size of about 30 nm with rather well defined grain boundaries.

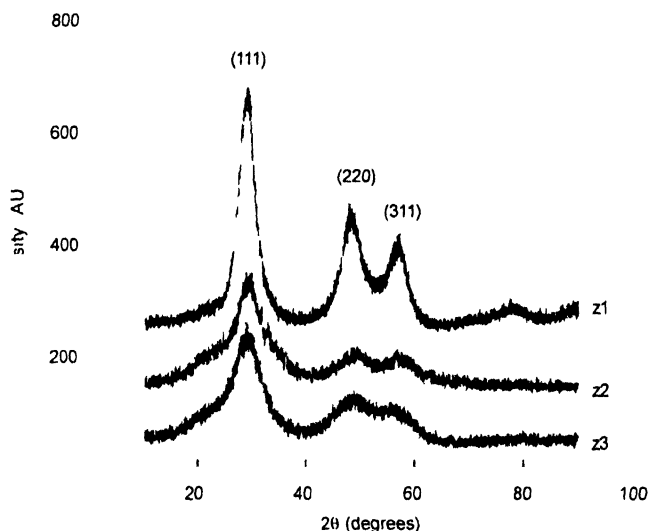


**Figure 1** XRD patterns of nanostructured crystals of ZnS (Z1) corresponds to ZnS prepared without capping agent (Z2) and (Z3) those with 0.001 M and 0.05 M mercaptoethanol as capping agent

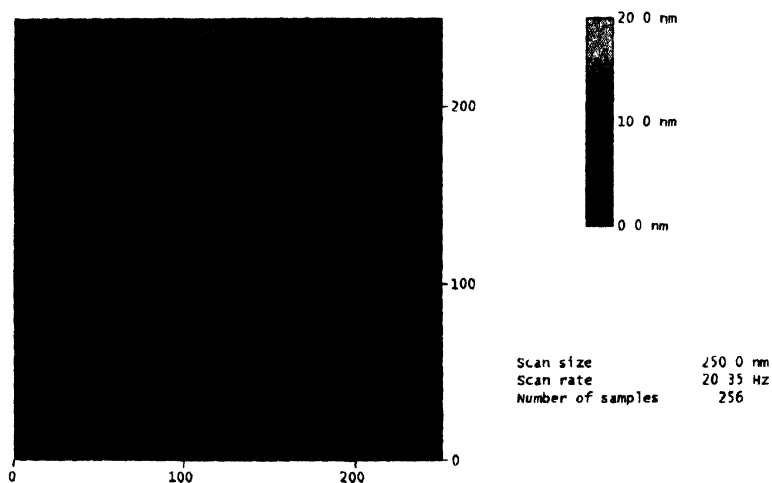


**Figure 2.** Two dimensional AFM image of pellet of dried nanocrystalline ZnS particles prepared with 0.001 M mercaptoethanol (Z2)

The optical absorbance of the Z1, Z2 and Z3 samples are shown in Figure 3. It is clearly seen from the figure that there is blue shift in the absorption edge of the optical spectra of ZnS as the particle size decreases due to the quantum confinement effect.

**Table 1.** Grain size of Z1, Z2 and Z3 samples obtained from XRD data and EMA and their band gaps

Sample	Grain size from XRD (nm)	Band gap (eV)	Grain size from EMA (nm)
Z1	2.9	3.6	
Z2	2.0	3.8	2.4
Z3	1.6	4.0	1.9

The band gap of the sample is calculated from the absorbance spectra shown in Figure 3 using the relation [25]  $(\alpha h\nu)^{1/n} = A(h\nu - E_g)$ , where  $\alpha$  is the absorption co-efficient,  $h\nu$  is the photon energy,  $A$  is a constant and  $E_g$  is the band gap of the material. The value of  $n$  in the exponent is 1/2 for direct, allowed transitions.

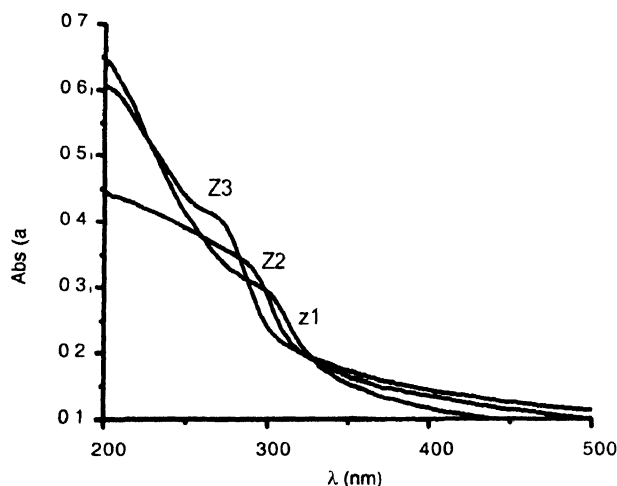
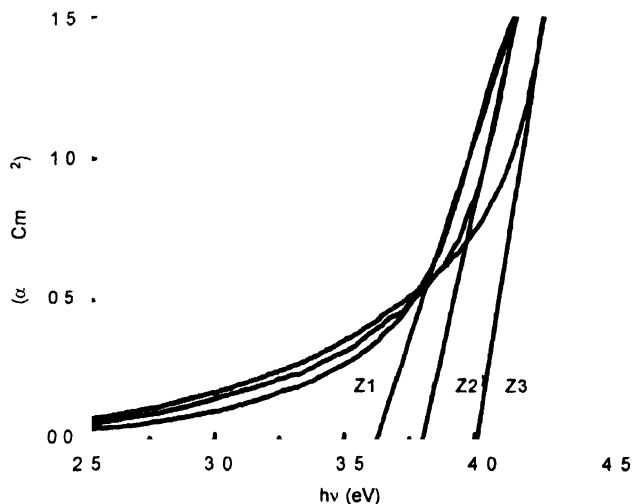
**Figure 3.** Absorbance spectra of thin films of nanocrystalline ZnS deposited on quartz substrate (Z1) corresponds to ZnS prepared without capping, (Z2) and (Z3) those with 0.001 M and 0.05 M capping

Figure 4 shows the plots of  $(\alpha h\nu)^2$  vs.  $h\nu$ . The linear portion of the plot of  $(\alpha h\nu)^2$  vs  $h\nu$  in the region of strong absorption has been extrapolated to obtain the intercept on the  $h\nu$  axis. The intercept gives the value of the band gap  $E_g$ , which is also listed in Table 1. It is clear that the band gap increases with decrease in particle size. From Table 1 it is also observed that optical bandgap of the particles Z2 and Z3 are found to exceed the bandgap 3.6 eV of bulk ZnS. This can be attributed to the quantum confinement effect as the particle size becomes smaller than the Bohr exciton radius (2.5 nm) of ZnS. The exciton energy  $E_s$  obtained using effective mass approximation (EMA) for strong confinement is given by [4]  $E_s = E_g + (\hbar^2 \pi^2) / (2\mu R^2) - (1.786e^2) / (4\pi\epsilon_0 \epsilon R) - 0.248 E_{Ry}^*$ , where  $\mu$  is the reduced effective mass,  $\epsilon$  is the dielectric constant of ZnS and  $\epsilon_0$  is the permittivity in vacuum,  $E_{Ry}^*$  is the effective Rydberg energy. Using this relation the

grain size of Z2 and Z3 are found to be 2.4 nm and 1.9 nm respectively (Table 1). The grain size determined from XRD data and EMA are found to agree.



**Figure 4.** Variation of  $(h\nu\alpha)^2$  vs  $h\nu$  of thin films of ZnS. The linear portion of the curves has been extrapolated to obtain the intercept to give the band gap of ZnS crystals. (Z1) corresponds to ZnS prepared without capping agent (Z2) and (Z3) those with 0.001 M and 0.05 M capping agent.

Figure 5 shows the variation of log resistivity ( $\ln \rho$ ) with the reciprocal of temperature  $1000/T$ . The resistivity  $\rho$  of Z1 shows a fairly large constant value over this temperature range, indicative of highly insulating nature. However, the resistivity of Z2 shows a transition at around 250 K and the linear fit of the curve of Z2 over the region of transition shows that it follows the Arrhenius equation  $\rho = \rho_0 \exp(E_a/kT)$ , where  $E_a$  is the thermal activation energy and  $k_B$  is the Boltzmann constant. The thermal activation energy of the

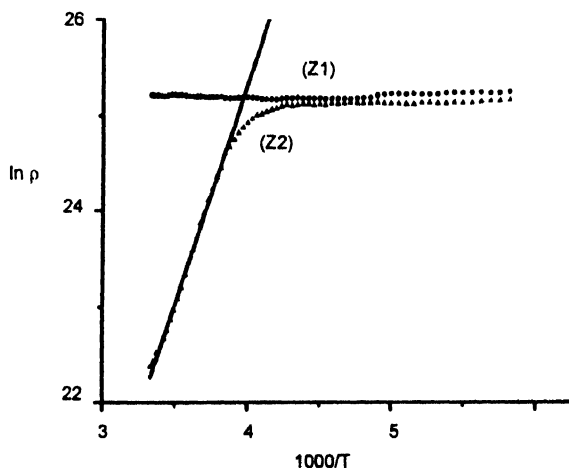


**Figure 5.** Variation of  $\ln \rho$  with  $1000/T$  of pellets of ZnS nanocrystals prepared without capping agent (Z1) and prepared with 0.001 M mercaptoethanol (Z2).

nanostructured ZnS crystals Z2 prepared using mercaptoethanol is then obtained from the slope of the linear portion of the curve of Z2. The value of  $E_a$  is found to be 0.4 eV, is much smaller than the band gap of 3.6 eV of bulk ZnS. Ion and Antohe [26] in their investigation of temperature dependence of electrical resistance of CdSe thin films placed in a He closed cycle cryostat reported the presence of a deep donor level located at 0.37 eV below the bottom edge of the conduction band. The present observed value of  $E_a$  of 0.4 eV is close to their reported value of CdSe thin films. To understand this better, we attempt to record the TL glow curves of these ZnS crystals both before and after  $\gamma$ -rays irradiation. However, no TL response is observed. It is interesting to note that electron or hole traps are produced in the band gaps of the nanocrystals even without irradiation since in such particles ions at the surface increase rapidly when the size becomes smaller [12,13]. Carriers trapped in such surface states may be released by thermal stimulation and recombine at recombination centers to give TL. Chen *et al* [12-13] observed TL of nanocrystalline ZnS samples, which has been attributed to the long wavelength peak in the absorbance spectrum and further to the presence of surface states. On the other hand, Kumbhojkar *et al* did not observe any red shifted peak in the absorption spectra of ZnS [9]. The thermal activation energy of 0.4 eV found from the present resistivity data may thus be associated with the charge carrier traps in the presence of the capping agent. The activation energy of 0.4 eV, being in the far infra-red region, is thus corroborated with absence of peak in UV-Visible absorption spectra and TL read out.

#### 4. Conclusion

Nanocrystalline ZnS particles both in powder and thin film have been prepared using wet chemical method. The sizes of crystallites are found to lie in the range of 1.6–2.9 nm. The optical and electrical properties have been studied. The quantum confinement effect is apparent from the observed blue shift of the absorption spectra. The band gap increases from 3.6 to 4.0 eV as the size decreases from 2.9 to 1.6 nm. Resistivity of pellets of nanocrystalline ZnS prepared with capping agent gives the thermal activation energy of 0.4 eV, which is associated with the formation of charge carrier traps in the presence of the capping agent.

#### Acknowledgment

One of the authors (WSS) wishes to thank the University Grants Commission, New Delhi for financial assistance [vide its letter F No. 30-5/2004(SR)]. We also would like to thank V. Ganesan and N. P. Lalla, UGC-DAE CSR, Indore for AFM and XRD measurements.

#### References

- [1] A. L. Efros and A. L. Efros *Phys. Semicond. Sov.* **16**, 772 (1982).
- [2] L. E. Brus *J. Phys. Chem.* **90**, 2555 (1986).
- [3] T. Trindade and P. N. L. Pickett O'Brien *Chem. Mater.* **13**, 3843 (2001).
- [4] A. D. Yoffe *Advances in Phys.* **42**, 173 (1993).
- [5] S. Mahamuni, A. A. Khosravi, M. Kundu, A. Kshirsagar, A. Badekar, D. B. Avasare, P. Singh and S. K. Kulkarni *J. Appl. Phys.* **73**, 5237 (1998).

- [6] K K Nanda, S N Sarangi, S Mohanty and S N Sahu *Thin Solid Films* **322** 21 (1998)
- [7] S N Bahera, S N Sahu and K K Nanda *Indian J Phys* **74A** 81 (2000)
- [8] L Brus *Appl Phys* **A53** 465 (1991)
- [9] N Kumbhojkar, V V Nikesh, A Kshirsagar and S Mahamuni *J Appl Phys* **88** 6260 (2000)
- [10] I K Battisha, H H Afify, G Fattah El Abd and Y Badr *Fizika* **11** 31 (2002)
- [11] T Ogata, H Hosokawa, T Oshiro, Y Wada, T Sakata, H Mori and S Yanagida *Chem Lett* **21** 1665 (1992)
- [12] W Chen, Z Wang, Z Lin and L Lin *J Appl Phys* **82** 3111 (1997)
- [13] W Chen, Z Wang, Z Lin and L Lin *Appl Phys Lett* **70** 1465 (1997)
- [14] S Banerjee, R Pal, A B Maity, S Chaudhuri and A K Pal *Nanostructured Materials* **3** 301 (1997)
- [15] A Osinsky, Y Qui, J Mahan, H Temkin, S A Gurevich, S I Nesterov, E M Tanklevskaia, V Tretyakov and O A Lavrova *Appl Phys Lett* **71** 509 (1997)
- [16] I O Oladeji and L Chow *Thin Solid Films* **474** 77 (2004)
- [17] S C Qu, W H Zhou, F Q Liu, N F Chen, Z G Wang, H Y Pan and D P Yu *Appl Phys Lett* **80** 3605 (2002)
- [18] I O Oladeji and L Chow *J Electrochem Soc* **144** 2342 (1997)
- [19] A Antony, K V Murali R Manoj and M K Jayaraj *Matt Chem and Phys* **90** 106 (2005)
- [20] P K Ghosh, M K Mitra and K K Chattopadhyay *Nanotechnology* **16** 107 (2005)
- [21] I O Oladeji and L Chow *Thin Solid Films* **339** 148 (1999)
- [22] A U Ubale and D K Kulkarni *Bull Mat Sc* **28** 43 (2005)
- [23] A Ashour, H H Afifi and S A Mahmoud *Thin Solid Films* **248** 253 (1994)
- [24] Ch Hammond *The Basis of Crystallography and Diffraction* (Oxford Oxford) p148 (1887)
- [25] J I Pankove *Optical Processes in semiconductors* (New Jersey, USA Prentice Hall) p34 (1971)
- [26] L ion and S Atohe *J Appl Phys* **97** 013513 (2005)